

See discussions, stats, and author profiles for this publication at: <https://www.researchgate.net/publication/231403928>

# Mesoscopic structure of pattern formation in initially uniform colloids

ARTICLE in THE JOURNAL OF PHYSICAL CHEMISTRY · OCTOBER 1982

Impact Factor: 2.78 · DOI: 10.1021/j100219a006

---

CITATIONS

18

---

READS

13

## 3 AUTHORS:



**Stefan C Müller**

Otto-von-Guericke-Universität Magdeburg

288 PUBLICATIONS 5,045 CITATIONS

SEE PROFILE



**Shoichi Kai**

Kyushu University

228 PUBLICATIONS 2,515 CITATIONS

SEE PROFILE



**John Ross**

Stanford University

89 PUBLICATIONS 2,467 CITATIONS

SEE PROFILE

# Mesoscopic Structure of Pattern Formation in Initially Uniform Colloids

Stefan C. Müller,<sup>†</sup> Sholchl Kai,<sup>‡</sup> and John Ross\*

Department of Chemistry, Stanford University, Stanford, California 94305 (Received: June 7, 1982; In Final Form: August 13, 1982)

Macroscopic inhomogeneities formed on a length scale of the order of 1 mm after many hours from an initially homogeneous colloid of lead iodide in an agar gel are shown to consist of dense regions of predominantly independent colloidal particles and empty regions. Some coagulation of colloidal particles occurs, but the structures are not formed by contiguous crystallites. The mesoscopic structure is determined from photographs taken with a microscope to a resolution of 1  $\mu\text{m}$ . The macroscopic length scale, the average radius of colloidal particles, and the average interparticle distance in the final pattern vary strongly with the initial supersaturation. The size distribution of colloidal particles is measured for one system. These observations support the hypothesis that the formation of such macroscopic inhomogeneities and periodic precipitation processes are the result of a chemical instability due to the coupling of autocatalytic growth of colloidal particles and diffusion.

An initially uniform colloid of appropriate total concentration of  $\text{PbI}_2$  develops in time visible, spatially non-uniform distributions of  $\text{PbI}_2$ .<sup>1-4</sup> These macroscopic inhomogeneities form irregular patterns on a length scale of the order of 1 mm. We report here measurements on the mesoscopic structure (to a resolution of about 1  $\mu\text{m}$ ) of these nonuniform distributions as determined by photographs taken with a light microscope. We find the dense regions of  $\text{PbI}_2$  to consist mostly of independent colloidal particles, but a small degree of coagulation of these particles is seen. The dense regions are separated by spaces essentially devoid of colloidal particles. The structures do not consist of contiguous crystallites.

In order to obtain macroscopic patterns in initially homogeneous salt solutions we dissolved a small amount of  $\text{PbI}_2$  (of the order of 5 mM) in water at 95 °C (the solubility of  $\text{PbI}_2$  at 95 °C is 8.6 mM); then we added 1% agar-agar gel. The solution was stirred until homogeneous and then poured into a preheated Petri dish (80 °C) to obtain a layer of solution of about 1 mm thickness. The dishes were covered, placed on an insulating material, and allowed to cool at room temperature (22 °C). After 1 h a gel forms and becomes uniformly yellow. Within the range of initial concentration of  $\text{PbI}_2$  from 4.8 to 6.6 mM the distribution of the salt becomes, after a time of several hours to 1 day (see Figure 1A), nonuniform and develops visible macroscopic spatial patterns. For initial concentrations outside this range, both lower and higher, the distribution of colloidal particles of  $\text{PbI}_2$  remains uniform. The dishes were left undisturbed for at least 2 days; after that time no further changes occurred in the distribution of  $\text{PbI}_2$ .

The macroscopic patterns were inspected with a light microscope. A sharp image was obtained for magnifications up to 200-fold, for which the size of the smallest discernible particle is of the order of 1  $\mu\text{m}$ .<sup>5</sup> The finite thickness of the gel layer (1–1.5 mm) did not allow for still higher magnification, which would require the distance between the objective lens and the sample to be smaller than 1.5 mm. The depth of field was approximately 100  $\mu\text{m}$  for the lowest magnification (28-fold) and 30  $\mu\text{m}$  at the

upper limit (190-fold). The vertical extent of the nearly two-dimensional patterns was usually less than 200  $\mu\text{m}$ . Some of the microscope pictures were investigated with a reticle (magnified six times) and the size of particles was measured within an error of  $\pm 0.1$  mm, which at 190-fold magnification corresponds to an error of  $\pm 0.5$   $\mu\text{m}$ .

Two examples of macroscopic pattern formation are presented in Figure 1A (system I) and Figure 2A (system II). The initial concentrations of  $\text{PbI}_2$  were 5.2 and 6.4 mM for systems I and II, respectively; these values correspond to supersaturation ratios  $S = 2.8$  (I) and  $S = 3.4$  (II), where  $S$  is the  $\text{PbI}_2$  concentration in units of the solubility (1.84 mM for  $\text{PbI}_2$  in water at 25 °C). The patterns can be roughly described as two-dimensional networks with a characteristic average pore size or length scale  $L$ , which ranges from 2 to 8 mm for system I and from 0.5 to 2 mm for system II. Microscope pictures with successively increasing magnification of selected regions are shown in parts B, C, and D of Figure 1 for system I and in parts B and C of Figure 2 for system II. The magnifications are indicated by scale bars and further specified in the captions. In both systems the visibly dense regions of  $\text{PbI}_2$  consist of a large number of essentially independent colloidal particles. The spaces separating dense regions of  $\text{PbI}_2$  are devoid of colloid except for a few relatively large particles (radius up to 20  $\mu\text{m}$ ), which are randomly distributed (Figures 1B and 2, B and C).

We made the following simple analysis of the mesoscopic structures. In system I, picture 1C, which covers an area of approximately 1 mm<sup>2</sup> of the pattern shown in Figure 1A, we selected a representative section; after further magnification (Figure 1D) we measured the radius  $R$  of each of the visible particles. The total number of particles in the sample,  $N_{\text{tot}}$ , is 590; the average radius is 4.3  $\mu\text{m}$ ; and the variance 2  $\mu\text{m}$ . The measured particle size distribution is shown in Figure 3; the dashed line was drawn by eye to fit the measured points. The largest radius in this plot is 10.5  $\mu\text{m}$ , but there are particles in system I with radius up to 12  $\mu\text{m}$  (Figure 1C) which do not appear in

<sup>†</sup> Present address: Max-Planck-Institut für Ernährungsphysiologie, D4600 Dortmund, West Germany.

<sup>‡</sup> Present address: Department of Electronics, Kyushu University, Fukuoka 812, Japan.

(1) M. Flicker and J. Ross, *J. Chem. Phys.*, **60**, 3458 (1974).  
 (2) J. Ross, *Ber. Bunsenges. Phys. Chem.*, **80**, 1112 (1976).  
 (3) D. Feinn, P. Ortoleva, W. Scaif, S. Schmidt, and M. Wolff, *J. Chem. Phys.*, **69**, 27 (1978).  
 (4) S. C. Müller, S. Kai, and J. Ross, *J. Phys. Chem.*, accepted for publication.

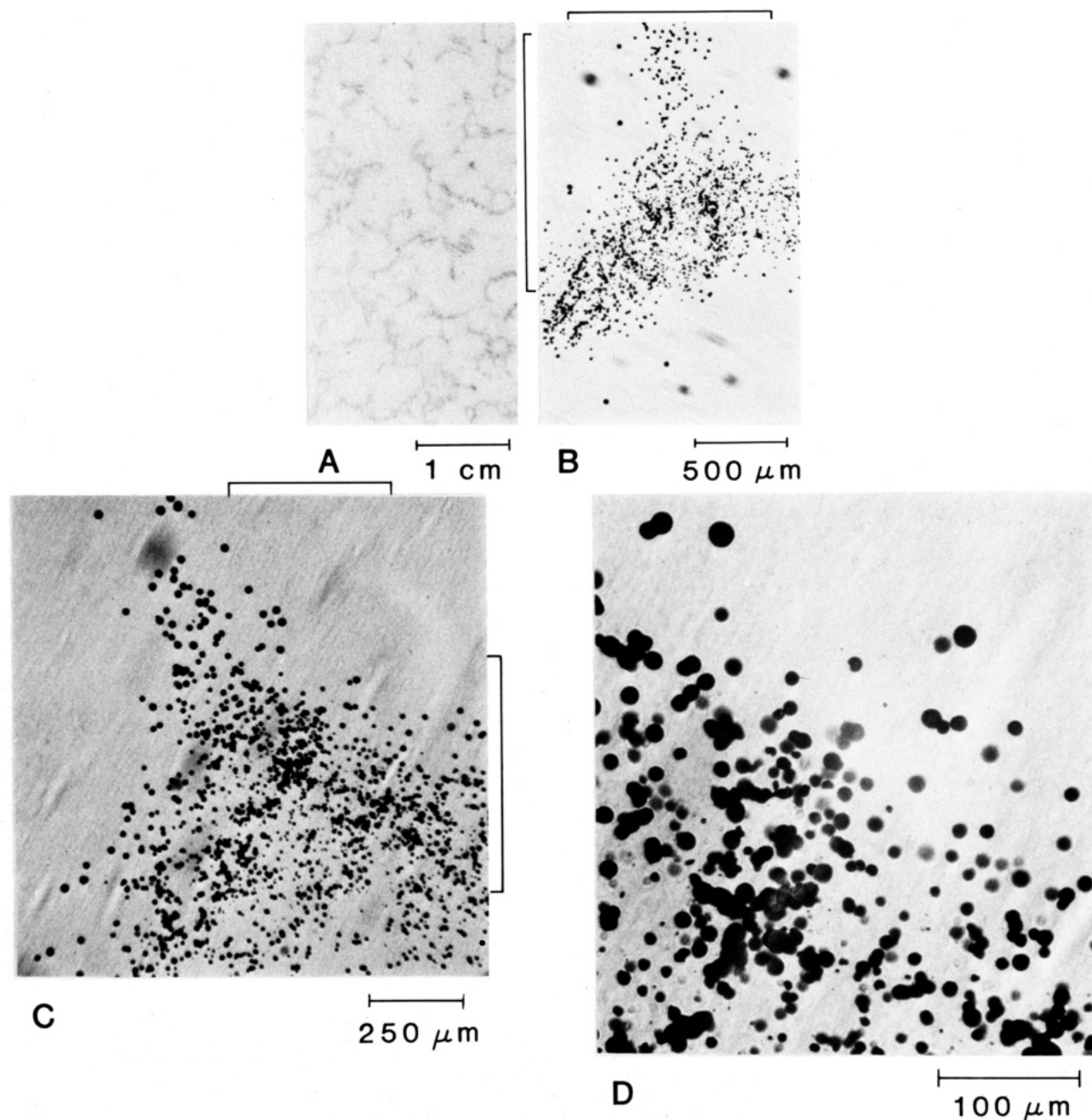


**Figure 1.** Pattern formation in system I after 1 week. Photograph of macroscopic inhomogeneities, 1.5 times enlarged (A), and microscope photographs of a part of (A) with magnification 28x (B), 58x (C), and 190x (D). The depth of field is 100  $\mu\text{m}$  in (B) and 30  $\mu\text{m}$  in (C) and (D). The pattern is formed primarily by unconnected particles. (B) and (C) show different but comparable regions of (A); the brackets in (B) mark the boundaries of an area of the size of (C). (D) shows a region of (C), as indicated by the brackets in (C).

Figure 1D. Particles with  $R < 1 \mu\text{m}$  appear on the picture as dots with  $R \approx 1 \mu\text{m}$ .<sup>5</sup> We observed only a small number of such dots which leads us to believe that only few of these particles are present.<sup>6</sup> An estimate of the average interparticle distance  $\langle D \rangle$  of the structure of Figure 1D, calculated according to the equation  $\langle D \rangle = [N_{\text{tot}}/(2A)]^{-1/2}$ , where  $A$  denotes the surface area, yields a value of 28  $\mu\text{m}$ .

Although many of the colloidal particles are independent

there are groups of particles which appear as small clusters. Some of these consist of independent colloidal particles in different planes located such that a two-dimensional projection gives the appearance of coagulation. However, there is evidence for coagulated particles which was obtained by illuminating the samples from the side. In Figure 4 we show a microscope picture of originally 190-fold magnification (system I), which was further enlarged by a factor of 3, the arrow in the figure points to a cluster.

A similar analysis of the mesoscopic structure of the dense region of  $\text{PbI}_2$  in system II, as shown in Figure 2C, is not possible because of insufficient spatial resolution, but some estimates can be made for the regions toward the edges of the structure, where particles are distinguishable. The largest particles there have a radius of 2.5  $\mu\text{m}$  and the average particle size is estimated to be  $\langle R \rangle \approx 0.8 \mu\text{m}$ . There appear to be many particles with  $R \leq 0.5 \mu\text{m}$ . The

(5) For the highest magnification used, particles of diameter 1  $\mu\text{m}$  are sharply imaged. Smaller particles indicate their presence by a blurred image of size of the order of 1  $\mu\text{m}$ .

(6) It would be interesting to obtain particle size distributions for various initial conditions. The shapes of such distributions are different for the case of diffusion-limited and reaction-limited colloidal growth; C. Wagner, *Z. Elektrochem.*, **65**, 581 (1961). The time scales of the growth of the structure rules out diffusion-limited kinetics, and the implications of that for a theoretical analysis are discussed in G. Venzl and J. Ross, *J. Chem. Phys.*, accepted for publication.

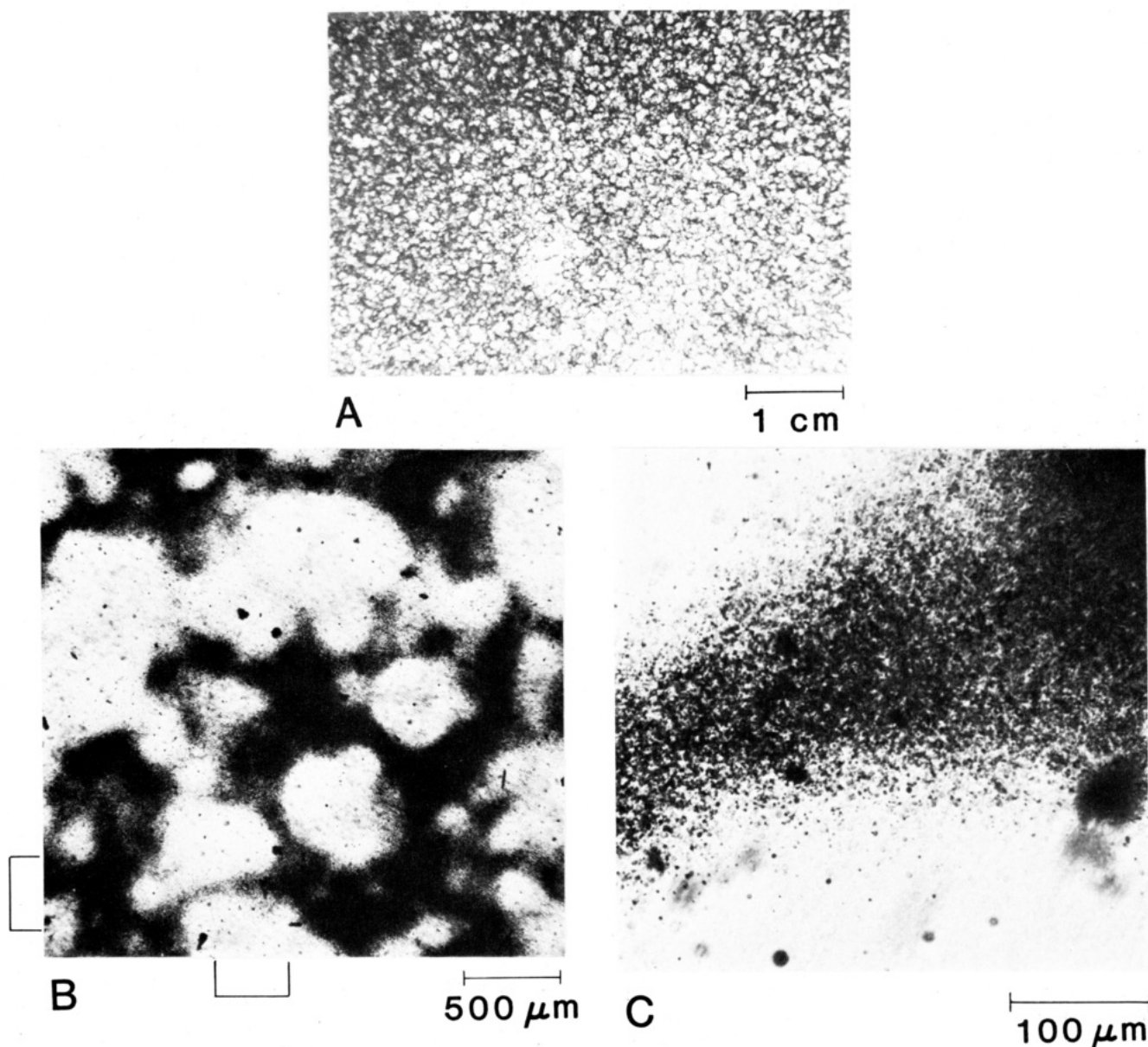


**Figure 2.** Pattern formation in system II after 1 week. Photograph of macroscopic inhomogeneities, 1.5 times enlarged (A), and microscope photographs of a part of (A) with magnification 28x (B) and 190x (C). The depth of field is 100  $\mu\text{m}$  in (B) and 30  $\mu\text{m}$  in (C). Unconnected particles can be seen in (C). The brackets in (B) indicate an area of the size of (C).

average interparticle distance  $\langle D \rangle$  is of the order of 6  $\mu\text{m}$ . No estimates can be given for the much denser inner regions of the structure. Coagulation cannot be separated from effects due to the two-dimensional projection, because the depth of the field of view ( $\approx 30 \mu\text{m}$ ) allows for several layers of particles to be sharply imaged.

Our results for the length scale of the macroscopic patterns  $L$ , the average particle sizes  $\langle R \rangle$ , and the average interparticle distances  $\langle D \rangle$  for systems I and II are summarized in Table I. The degree of the initial supersaturation is given by the quantity  $S - 1$ . We deduce from these results that an increase in the  $\text{PbI}_2$  concentration and consequently in the degree of supersaturation ( $S - 1$ ) results in a pronounced decrease in particle size and interparticle distance. There is evidence that the number of initial nuclei is larger for high than for low supersaturations.<sup>7</sup> We find a strong correlation between the macroscopic and mesoscopic features of the two investigated

patterns: each of the quantities  $L$ ,  $\langle R \rangle$ , and  $\langle D \rangle$  is decreased by about the same factor  $5 (\pm 2)$ , when  $S - 1$  is increased from 1.8 to 2.4. The substantial, and similar, change in all of the observed length scales of the structures is brought about by altering  $S - 1$  by only a factor of 1.33. This suggests that the role of supersaturation in determining the length scales of pattern formation in initially uniform colloids is characterized by a power law for  $S - 1$  with an exponent larger than 5.

The theory of the macroscopic structure formation in initially uniform colloids is based on the hypothesis of the occurrence of a chemical instability.<sup>1,3,8,9</sup> Consider a spatially uniform distribution of colloidal particles past the nucleation stage. The solubility of a colloidal particle depends on its size due to the positive surface Gibbs free energy contribution.<sup>10</sup> If, by a natural fluctuation or applied perturbation, some particles grow larger than their neighbors, then a spatial gradient (of  $\text{PbI}_2$ ) is established and the larger particles grow still further at the expense of the smaller neighbors (Ostwald ripening). The kinetics of this autocatalytic growth of colloidal particles, coupled

(7) L. B. Allen and J. Kassner, *J. Colloid Interface Sci.*, **30**, 81 (1969).

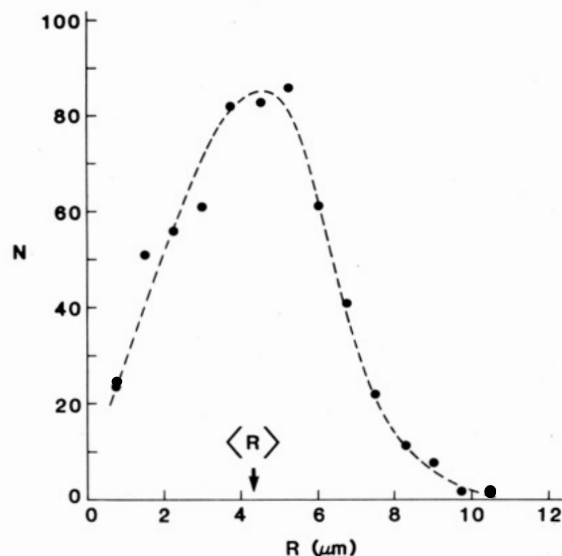


**Figure 3.** Size distribution of the particles shown in Figure 1D (system I). The number of particles  $N$  of radius  $R$  is plotted vs.  $R$  for discrete intervals of  $R$  of width  $0.75 \mu\text{m}$ . The average value of  $R$  is indicated by the arrow. The dashed line is drawn by eye to fit the measured points.

with diffusion, leads to equations which give rise to the formation of macroscopic structures.<sup>2,3,5,11</sup> The observation that the structures consist primarily of regions of independent colloidal particles and spaces devoid of colloidal particles, rather than structures formed by coagulation or epitaxial growth, supports the theory based on a chemical instability. The theory is also applicable to conditions in which concentration gradients exist initially<sup>9</sup> (Liesegang rings).

(8) R. Lovett, P. Ortoleva, and J. Ross, *J. Chem. Phys.*, **69**, 947 (1978).

(9) S. Kai, S. C. Müller, and J. Ross, *J. Chem. Phys.*, **76**, 1392 (1982).

(10) I. M. Lifshitz and V. V. Slyozov, *Phys. Chem. Solids*, **19**, 35 (1961).

(11) G. Venzl and J. Ross, *J. Chem. Phys.*, accepted for publication.

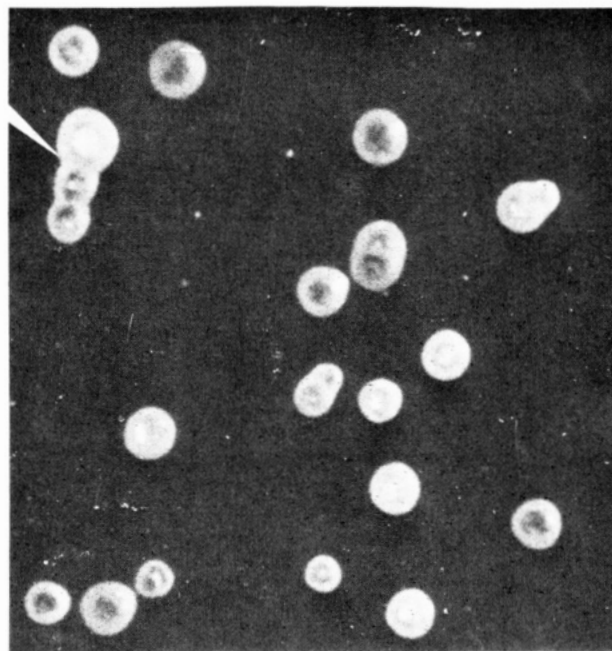


**Figure 4.** An arrow points to clusters of coagulated particles in system I. The microscope photograph of originally 190-fold magnification is enlarged by a factor of 3. The sample was illuminated from the side.

**TABLE I:** Initial Concentration of Lead Iodide  $c$ ; Degree of Supersaturation ( $S - 1$ ); Length Scale of Macroscopic Pattern  $L$ ; Maximum, Minimum, and an Average Value for Particle Radius ( $R_{\text{max}}$ ,  $R_{\text{min}}$ ,  $\langle R \rangle$ ); and Average Interparticle Distance ( $D$ ) for Systems I and II

sys- tem	$c$ , mM	$S - 1$	$L$ , mm	$R_{\text{min}}$ , $\mu\text{m}$	$R_{\text{max}}$ , $\mu\text{m}$	$\langle R \rangle$ , $\mu\text{m}$	$\langle D \rangle$ , $\mu\text{m}$
I	5.2	1.8	2-8	0.8	12	4.3	28
II	6.4	2.4	0.5-2	$\leq 0.5$	2.5	$\approx 0.8$	6

**Acknowledgment.** We thank Dr. D. Kumamoto for helpful discussions. This work was supported in part by the National Science Foundation and by the Air Force Office of Scientific Research.